Reactions of Co-ordinated Ligands. Part 45.[1] Ligand Displacement and Oxidative Reactions of the Carbyne Complex $[Mo(\equiv CCH_2Bu^t)\{P(OMe)_3\}_2(\eta\text{-}C_5H_5)]$; Crystal and Molecular Structures of $[Mo\{\eta^3\text{-}RN{=}C\cdots C(CH_2Bu^t)\cdots C{=}NR\}(CNR)_2(\eta\text{-}C_5H_5)]$(R = 2, 6-$Me_2C_6H_3$), $[Mo(C{=}CHBu^t)I\{P(OMe)_3\}_2(\eta\text{-}C_5H_5)]$, and $[\overset{\frown}{M}o\{{=}C(CH_2Bu^t)P(O)(OMe)_2\}\{P(OMe)_3\}(\eta\text{-}C_5H_5)]$†

Paul K. Baker, Geoffrey K. Barker, Daljit S. Gill, Michael Green,* A. Guy Orpen, and Ian D. Williams
Department of Inorganic Chemistry, University of Bristol, Bristol BS8 1TS
Alan J. Welch
Department of Chemistry, University of Edinburgh, Edinburgh EH9 3JJ

Reaction of the carbyne complexes $[M(\equiv CCH_2R)\{P(OMe)_3\}_2(\eta\text{-}C_5H_5)]$(M = Mo or W, R = Bu^t or Pr^i) with 2,6-xylyl isocyanide affords the complexes $[M\{\eta^3\text{-}R'N{=}C\cdots C(CH_2Bu^t)\cdots C{=}NR'\}(CNR')_2(\eta\text{-}C_5H_5)]$(R' = 2,6-$Me_2C_6H_3$), the molybdenum complex being identified by *X*-ray crystallography. In the 1,3-di-imino-substituted η^3-allyl fragment the nitrogen atoms are bent back away from the allyl plane to subtend C–C–N angles of 135.2(9) and 133.1 (9)°. The central carbon atom of the allyl is also tilted away from the metal possibly due to intramolecular interactions. These complexes show temperature-dependent n.m.r. spectra which are discussed in terms of rotation about C–NR bonds and *endo/exo* isomerism. In attempting to understand the mechanism of formation of these complexes the solution $^{31}P\text{-}\{^1H\}$ n.m.r. spectra of the carbyne in the presence of free $P(OMe)_3$ was studied. A DANTE pulse sequence suggested that dissociative loss of $P(OMe)_3$ is not a rate-determining step in the reaction with isocyanide. The reaction of $[Mo(\equiv CCH_2Bu^t)\{P(OMe)_3\}_2(\eta\text{-}C_5H_5)]$ with CO was also studied leading to loss of $P(OMe)_3$, and formation of $[Mo(\equiv CCH_2Bu^t)(CO)\{P(OMe)_3\}(\eta\text{-}C_5H_5)]$, $[Mo(\equiv CCH_2Bu^t)(CO)_2(\eta\text{-}C_5H_5)]$, and $[Mo\{\sigma\text{-}CH(CO_2Me)CH_2Bu^t\}(CO)_2\{P(OMe)_3\}(\eta\text{-}C_5H_5)]$. The mechanism of formation of these complexes is discussed. In addition the reaction of potential one-electron oxidants with $[Mo(\equiv CCH_2Bu^t)\{P(OMe)_3\}_2(\eta\text{-}C_5H_5)]$ has been examined. Treatment with $[4\text{-}FC_6H_4N_2][BF_4]$ affords the vinylidene complex $[Mo(C{=}CHBu^t)(N_2C_6H_4Me\text{-}4)\{P(OMe)_3\}(\eta\text{-}C_5H_5)]$, whereas reaction with CF_3I gives the *X*-ray crystallographically identified complexes $[Mo(C{=}CHBu^t)I\{P(OMe)_3\}_2(\eta\text{-}C_5H_5)]$ and $[\overset{\frown}{M}o\{{=}C(CH_2Bu^t)P(O)(OMe)_2\}I\{P(OMe)_3\}(\eta\text{-}C_5H_5)]$. It is suggested that the latter complex is formed *via* the migration of a phosphonate group from molybdenum onto a carbyne carbon atom.

Our observation[2] that carbyne complexes of the type $[M(\equiv CCH_2Bu^t)\{P(OMe)_3\}_2(\eta^5\text{-}C_mH_n)]$(M = Mo or W; $m = n = 5$; $m = 9$, $n = 7$) can be synthesised by thermolysis of the σ-vinyl complexes $[M\{\sigma\text{-}(E)\text{-}CH{=}CHBu^t\}\{P(OMe)_3\}_3(\eta^5\text{-}C_mH_n)]$ provided an opportunity to compare the reactivity of these electron-rich molecules with the well known Fischer carbonyl carbyne[3] complexes. We have previously[1,4] reported on protonation reactions of these electron-rich systems, and in this paper we describe a detailed[5,6] study of trimethyl phosphite ligand-displacement reactions by 2,6-xylyl isocyanide and carbon monoxide, and also oxidative reactions with $[4\text{-}FC_6H_4N_2][BF_4]$ and R_FI ($R_F = CF_3$ or C_3F_7).

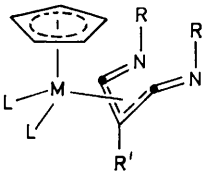

	M	R'
(**4**)	Mo	CH_2Bu^t
(**5**)	W	CH_2Bu^t
(**6**)	Mo	CH_2Pr^i

R = $C_6H_3Me_2$—2,6 L = σ—$CNC_6H_3Me_2$—2,6

Results and Discussion

Early studies by Fischer *et al.*[7] of the reaction of the carbyne complex *trans*-$[M(\equiv CPh)Br(CO)_4]$(M = Cr or W) with Bu^tNC established that one carbonyl ligand can be readily substituted by an isocyanide ligand, whereas the cationic carbyne complex $[Mn(\equiv CPh)(CO)_2(\eta\text{-}C_5H_5)][BF_4]$ forms an unstable ionic species formulated[8] as $[Mn\{C(Ph)CNBu^t\}(CO)_2(\eta\text{-}C_5H_5)][BF_4]$. In contrast, 2,6-xylyl isocyanide reacted at room temperature with a diethyl ether solution of $[M(\equiv CCH_2Bu^t)\{P(OMe)_3\}_2(\eta\text{-}C_5H_5)]$ [M = Mo (**1**) or W (**2**)] and $[Mo(\equiv CCH_2Pr^i)\{P(OMe)_3\}_2(\eta\text{-}C_5H_5)]$ (**3**) to give the orange-red crystalline products (**4**), (**5**), and (**6**) respectively; these were

* Present address: Department of Chemistry, King's College London, Strand, London WC2R 2LS.

† [η-1,3-Bis(2′,6′-xylylimino)-2-t-butylmethylallyl]η-cyclopentadienylbis(2,6-xylyl isocyanide))molybdenum, η-cyclopentadienyliodo(t-butylvinylidene)bis(trimethyl phosphite)molybdenum, and η-cyclopentadienyl[(dimethoxyphosphonyl)t-butylmethylmethylene-*CO*]-iodo(trimethyl phosphite)molybdenum.

Supplementary data available: see Instructions for Authors, *J. Chem. Soc., Dalton Trans.*, 1989, Issue 1, pp. xvii—xx.

Non-S.I. unit employed: atm = 101 325 Pa.

Table 1. Bond distances (Å) and selected interbond angles (°) in complex (**4**), CS atoms are C atoms of solvent

Mo–C(101)	2.326(11)	C(22)–C(221)	1.528(15)
Mo–C(102)	2.326(11)	C(3)–N(3)	1.178(14)
Mo–C(103)	2.349(11)	N(3)–C(31)	1.381(12)
Mo–C(104)	2.363(11)	C(36)–C(361)	1.544(17)
Mo–C(105)	2.349(11)	C(32)–C(321)	1.520(18)
Mo–C(1)	2.053(10)	C(4)–N(4)	1.267(12)
Mo–C(2)	2.164(9)	C(4)–C(5)	1.446(13)
Mo–C(3)	2.035(10)	N(4)–C(41)	1.420(12)
Mo–C(4)	2.163(10)	C(46)–C(461)	1.534(17)
Mo–C(5)	2.295(9)	C(42)–C(421)	1.523(18)
C(1)–N(1)	1.171(13)	C(5)–C(6)	1.521(14)
N(1)–C(11)	1.388(12)	C(6)–C(61)	1.545(15)
C(16)–C(161)	1.534(19)	C(61)–C(611)	1.563(19)
C(12)–C(121)	1.533(15)	C(61)–C(612)	1.551(19)
C(2)–N(2)	1.273(12)	C(61)–C(613)	1.545(20)
C(2)–C(5)	1.425(13)	CS(1)–CS(1′)	1.22(10)
N(2)–C(21)	1.420(11)	CS(1)–CS(2)	1.28(11)
C(26)–C(261)	1.542(16)	CS(2)–CS(3)	1.27(11)
C(1)–Mo–C(3)	83.1(4)	C(3)–N(3)–C(31)	171.3(11)
Mo–C(1)–N(1)	176.9(9)	N(4)–C(4)–C(5)	133.1(9)
C(1)–N(1)–C(11)	169.0(10)	C(4)–N(4)–C(41)	123.1(8)
N(2)–C(2)–C(5)	135.2(9)	C(2)–C(5)–C(4)	104.3(8)
C(2)–N(2)–C(21)	122.5(8)	C(5)–C(6)–C(61)	116.5(8)
Mo–C(3)–N(3)	175.8(9)		

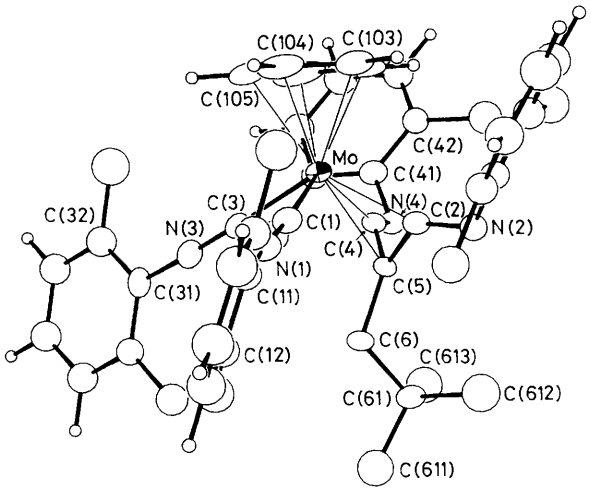

Figure 1. Molecular structure of complex (**4**); atoms are drawn to enclose 30% probability density. Methyl and methylene group hydrogen atoms have been omitted for clarity

isolated by column chromatography and crystallisation. Elemental analyses, i.r. and n.m.r. spectroscopy showed that similar reactions had taken place with all three carbyne complexes and that both trimethyl phosphite ligands had been displaced. Moreover, in addition to terminal isocyanide stretching frequencies the i.r. spectrum of, for example, (**3**) showed bands at 1 730br, m and 1 590s cm^{-1} implying the presence of a RN=C system formed by coupling of the isocyanide with the carbyne. In order to confirm this and to clarify the nature of these reactions an *X*-ray crystallographic study was carried out on suitable crystals of complex (**4**) grown from n-hexane; the crystals contained a non-stoicheiometric amount of solvent occluded in the lattice.

The molecular structure of (**4**) is shown in Figure 1 with selected bond lengths and angles listed in Table 1. This confirmed that both trimethyl phosphite ligands had been displaced and that two molecules of 2,6-xylyl isocyanide had combined with the CCH_2Bu^t carbyne fragment to form a 1,3-di-imino-substituted η^3-allyl system. The complex has effective C_s symmetry and an *endo* stereochemistry. Parameters within the C_5H_5 and the two terminally bonded 2,6-xylyl isocyanide ligands are unexceptional, but the geometry and mode of co-ordination of the allyl moiety are of interest. To our knowledge this study is the first structural characterisation of an allyl ligand where the terminal carbons are bonded to only one other atom, *i.e.* the 2,6-dimethylphenylimino-nitrogens, N(2) and N(4). These nitrogen atoms are bent back away from the allyl plane to subtend C–C–N angles of 135.2(9) and 133.1(9)°. Significantly greater bend back of the corresponding angles has been observed [9] in the iron complex $[Fe(CNBu^t)_3\{1—4\text{-}\eta\text{-}C(=NBu^t)=C(Ph)C(Ph)=C(=NBu^t)\}]$ where the adoption of transoid geometries about the C=N double bonds presumably minimises intra-ligand steric congestion. The central carbon atom is tilted away such that Mo-C(central) exceeds Mo-C(terminal) by *ca.* 0.13 Å. In η^3-allyl complexes generally,[10] and $[M(\eta^3\text{-allyl})L_2(\eta\text{-}C_5H_5)]$ complexes specifically,[11] either the reverse pattern is observed or there is no significant difference in M–C lengths. In complex (**4**) it is likely that the tilting away from the molybdenum is due in part to intramolecular repulsive interactions between the CH_2Bu^t group on C(5) and the aryl methyl groups of the terminally bonded isocyanide ligands.

With the establishment of the solid-state structure of complex (**4**) it was possible to interpret the solution n.m.r. spectra of (**4**)—(**6**). The room-temperature ^1H n.m.r. spectrum of (**4**) was consistent with the structure established in the solid state, *i.e.* an *endo*-orientated system, showing two inequivalent methyl groups attributable to the 2,6-dimethylphenylimino fragments of the η^3-RN=C···C(CH_2Bu^t)···C=NR ligand. This implied that there was hindered rotation about the C–N bonds, however, on warming to 44 °C coalescence of the two singlets at 2.07 and 2.05 occurred allowing the derivation of a free-energy barrier to rotation of 68.0 ± 0.5 kJ mol^{-1}. In contrast, the ^1H n.m.r. spectrum of the tungsten analogue (**5**) measured at room temperature showed only one 2,6-dimethylphenylimino methyl environment of a presumed *endo* isomer, and only on cooling to −70 °C were two methyl singlets observed at 2.01 and 2.00 with a $\Delta G^{\ddagger}_{T_c}$ value for rotation about the C–NR bond of 55.0 ± 0.5 kJ mol^{-1}. The isopropyl-substituted complex (**6**) also shows dynamic behaviour in solution, the ^1H n.m.r. spectrum at room temperature exhibiting signals due to both *endo* and *exo* isomers (2:1) (Scheme 1). However, on cooling to −50 °C only three methyl singlets were observed suggesting that whilst at this temperature rotation about the C–NR bonds of the *endo* isomer is frozen ($\Delta G^{\ddagger}_{T_c}$ 54.0 ± 0.5 kJ mol^{-1}) there is still free rotation about the C–NR bond of the *exo* isomer. Examination of Scheme 1 suggests that this difference in behaviour could be due in part to greater steric congestion in the *endo* isomer. It is more difficult to rationalise the differences in $\Delta G^{\ddagger}_{T_c}$ values for C–NR bond rotation of complexes (**4**) and (**5**), however it is possible that small M-allyl bond-length changes lower steric congestion slightly.

With an understanding of the structures of (**4**)—(**6**), consideration can be given to the possible reaction paths involved in their formation. Examination of the n.m.r. spectra of a solution of complex (**1**) in CD_2Cl_2 on addition of 1—4 equivalents of 2,6-xylyl isocyanide was revealing. The $^{31}P\text{-}\{^1H\}$ and ^1H n.m.r. spectra recorded on addition of 1 equivalent of 2,6-xylyl isocyanide showed the presence of free trimethyl phosphite and resonances attributable to $[Mo(\equiv CCH_2Bu^t)(CNC_6H_3Me_2\text{-}2,6)\{P(OMe)_3\}(\eta\text{-}C_5H_5)]$. Addition of a second equivalent of the isocyanide led to the liberation of a further molecule of $P(OMe)_3$ and the formation of a new carbyne complex presumed (i.r., n.m.r. spectroscopy) to be $[Mo(\equiv CCH_2Bu^t)(CNC_6H_3Me_2\text{-}2,6)_2(\eta\text{-}C_5H_5)]$. Only on addition of further equivalents of isocyanide were resonances observed due to the

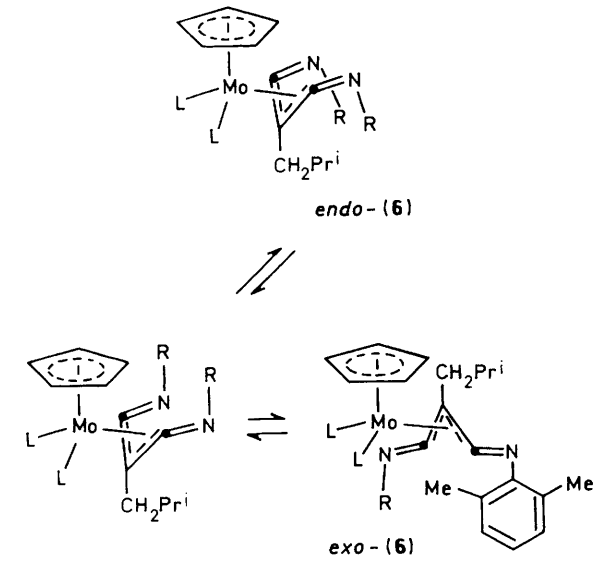

Scheme 1. L = σ-$CNC_6H_3Me_2$-2,6, R = 2,6-$Me_2C_6H_3$

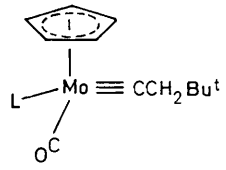

(7) L = $P(OMe)_3$
(8) L = CO

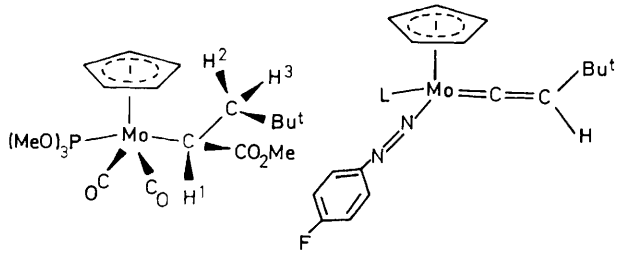

(9) (10) L = $P(OMe)_3$

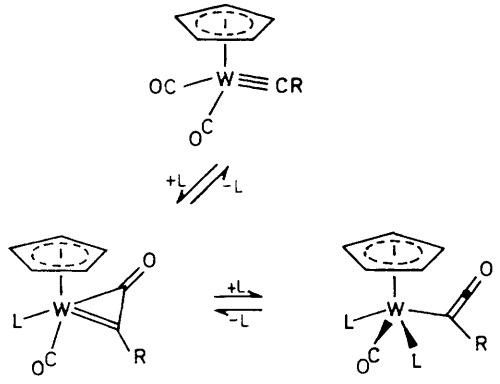

Scheme 2. R = Ph or C_6H_4Me-4; L = PMe_3 or PPh_3

isolated product (**4**). Because the carbyne complex (**4**) is an 18-electron system, the obvious reaction path for replacement of trimethyl phosphite by 2,6-xylyl isocyanide is *via* dissociative loss of $P(OMe)_3$ followed by capture by isocyanide of the co-ordinatively unsaturated species [Mo(≡CCH_2Bu^t){$P(OMe)_3$}-(η-C_5H_5)].

With a view to confirming this idea, the ^{31}P-{^1H} n.m.r. spectra of a solution of (**1**) in deuteriotoluene containing free trimethyl phosphite were recorded at different temperatures. Small differences in the chemical shifts of the two signals were observed due to change in temperature, but no broadening of the co-ordinated trimethyl phosphite signal was observed, even at 100 °C. Thus, any exchange between free and co-ordinated $P(OMe)_3$ was indicated to take longer than 0.5 s. An attempt was then made to observe even slower exchange by applying the DANTE pulse sequence of Morris and Freeman.[12] The studies were carried out on a sample containing the complex (**4**), free trimethyl phosphite, and free trimethyl phosphate contained in a sealed n.m.r. tube in deuteriotoluene as solvent at 100 °C. The latter species was added as a reference and should only have produced one ^{31}P-{^1H} resonance, however resonances were observed at −6.2 and 0.9 p.p.m. This was probably due to a hydrolysis product of trimethyl phosphate which is readily attacked by water. This did not affect the experiment, however, and both signals were utilised as references for measuring changes in the intensity of the co-ordinated $P(OMe)_3$ signal at 212.3 p.p.m. The spins of the free trimethyl phosphite were selectively inverted by a 180° pulse and the spectrum of the sample was then measured after a delay time, $0.1 < t < 2$ s. The fact that the relaxation time of free $P(OMe)_3$ is 1.4 s made the measurement of spectra after longer delay periods impossible. No reduction in the intensity of the co-ordinated $P(OMe)_3$ signal, relative to the reference, was observed indicating that the half-life for the exchange must be greater than *ca.* 10 s at +100 °C. Thus, these observations suggest that the room-temperature formation of complex (**4**) [and by analogy (**5**) and (**6**)] does not involve the initial dissociative loss of trimethyl phosphite.

An additional insight into these unusual coupling reactions came from a study of the effect of pressurising (300 atm) a solution of complex (**1**) in hexane with carbon monoxide. After 3 d at room temperature the resulting reaction mixture was separated by column chromatography. Elution with hexane–diethyl ether gave unreacted (**1**) together with three products (**7**), (**8**), and (**9**), isolated in yields of 31, 26, and 8% respectively. Elemental analysis, i.r. and n.m.r. spectroscopy showed that whilst (**7**) and (**8**) were simple carbonyl-substituted carbyne complexes with the structures illustrated, the minor product (**9**) was a carbomethoxy-substituted species. As with the isocyanide reactions, the lack of lability of the trimethyl phosphite ligands in (**1**) poses the problem as to how (**7**) and (**8**) are formed. The formation of (**9**) suggests, however, an interesting relationship with the reactions summarised in Scheme 2, and reported by Kreissl and co-workers.[13] Thus, treatment of tungsten carbyne complexes with phosphines can lead to the formation of η^2(3e)-ketenyl (metallacyclopropenone) complexes which can react further to give isolable σ(1e)-ketenyl complexes. This last step has an analogy with the η^2(3e) to σ(1e) transformation of the related η^2-vinyl complexes.[14–16] These reactions suggested that the formation of (**9**) might involve the capture by methanol (formed by hydrolysis of trimethyl phosphite) of the σ(1e)-ketenyl species (**C**) shown in Scheme 3, which is formed by the η^2(3e) to σ(1e) isomerisation of (**B**). Because of the relationship with the reactions shown in Scheme 2 it is reasonable to suggest that the η^2(3e)-ketenyl (**B**) could be formed by reaction of CO with (**7**), the carbon monoxide promoting migratory addition to the molybdenum–carbon triple bond.

This pathway cannot, however, be extended to explain the

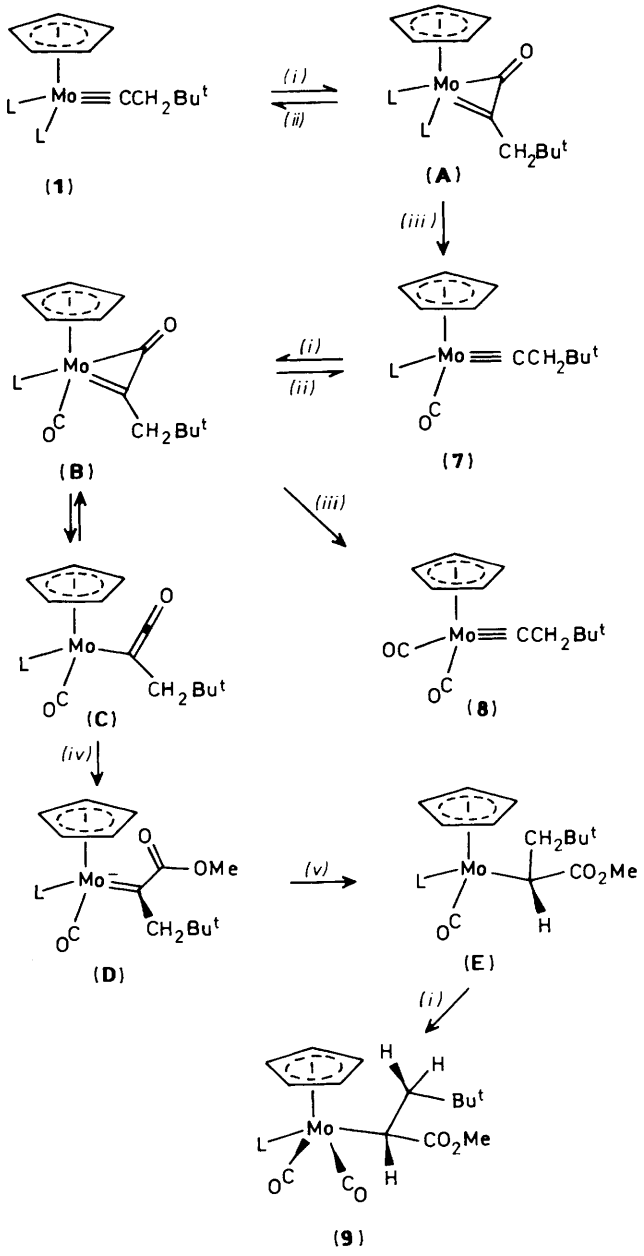

Scheme 3. L = $P(OMe)_3$. (*i*) + CO; (*ii*) −CO; (*iii*) −L; (*iv*) + MeO^-; (*v*) + H^+

formation of complex (**7**) from (**1**) because of the absence of co-ordinated carbon monoxide ligands. Consideration of the isolobal relationship CR $\longleftrightarrow$ $MoL_2(\eta\text{-}C_5H_5)$[17] suggests an alternative and possibly competitive path for both the transformation of (**1**) to (**7**) and for the step (**7**) to (**B**) (in Scheme 3). On thermolysis cyclopropenes undergo a chelotropic fragmentation reaction forming an alkyne and carbon monoxide.[18] Thus, in view of the relationship between (**1**) and an alkyne, and by invoking the principle of microscopic reversibility, carbon monoxide could react directly with (**1**) in a chelotropic type of reaction to form the η^2(3e)-ketenyl complex (**A**) (Scheme 3). Then following the reverse of the reaction path traversed in the Kreissl reaction, *i.e.* carbyne to η^2(3e)-ketenyl, the carbon monoxide, which is part of the η^2-ketenyl fragment in (**A**), could migrate onto the molybdenum with concomitant formation of a terminally bonded carbonyl ligand and dissociative loss of

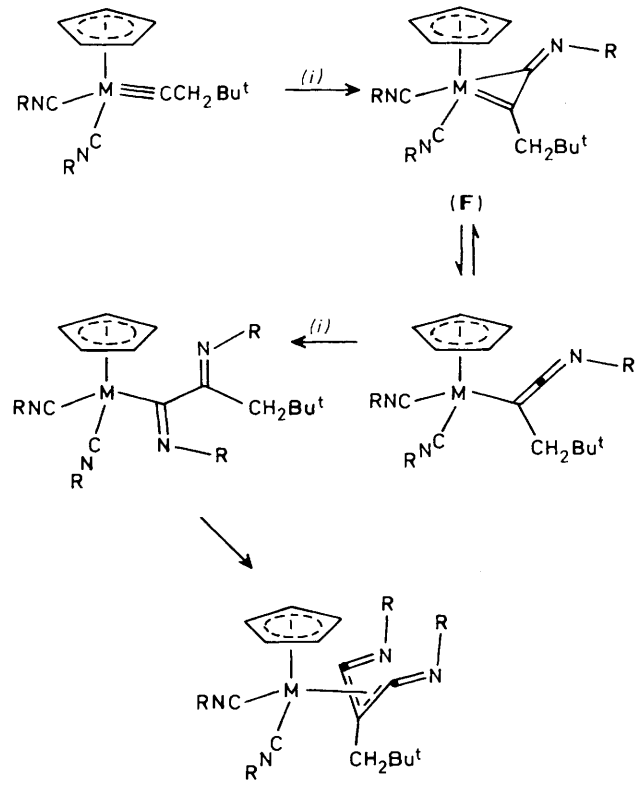

Scheme 4. M = Mo or W; R = 2,6-$Me_2C_6H_3$. (*i*) + $CNC_6H_3Me_2$-2,6

$P(OMe)_3$. A similar sequence of reactions provides an alternative path from complex (**7**) to (**B**). Although in the formation of an alkyne from a cyclopropenone both σ bonds to the CO are presumed to break simultaneously, in the reaction of carbon monoxide, for example, with (**7**), because of the asymmetric nature of the Mo≡C bond, it is likely that σ-bond formation to the carbyne carbon atom is more advanced than that to the molybdenum, and therefore the transition state approaches a σ(1e)-ketenyl, *i.e.* intermediate (**C**) in Scheme 3, rather than (**B**). Returning to the problem of how (**4**)—(**6**) are formed from 2,6-xylyl isocyanide and (**1**), the above discussion suggests that the intermediates $[M(\equiv CCH_2Bu^t)(CNC_6H_3Me_2\text{-}2,6)\{P(OMe)_3\}(\eta\text{-}C_5H_5)]$ and $[M(\equiv CCH_2Bu^t)(CNC_6H_3Me\text{-}2,6)_2(\eta\text{-}C_5H_5)]$(M = Mo or W) could be generated *via* a related chelotropic addition of the isocyanide to the Mo≡C bond of (**1**). This could then be followed by loss of trimethyl phosphite and migration of the isocyanide from a bridging mode between the metal and the original carbyne contact carbon to a σ-bonding mode. Repetition of the chelotropic reaction with the monophosphite complex would then afford the bis-σ-bonded isocyanide complex $[M(\equiv CCH_2Bu^t)(CNC_6H_3Me_2\text{-}2,6)_2(\eta\text{-}C_5H_5)]$. Then as is shown in Scheme 4 the intermediate (**F**) could be formed either by a chelotropic addition of isocyanide or by a Kreissl-type reaction, *i.e.* migratory addition of an already co-ordinated isocyanide to a bridging $\overline{MC(=NR)CCH_2Bu^t}$ mode. An insertion reaction must then intervene (Scheme 4) leading to the formation of the di-imino-substituted allyls (**4**)—(**6**). It is particularly interesting that related chemistry is not observed with the CO reaction and that the molecule $[Mo\{\eta^3\text{-}O{=}C{=}C(CH_2Bu^t){=}C{=}O\}(CO)_2(\eta\text{-}C_5H_5)]$ is not generated *via* a similar sequence of reactions with carbon monoxide.

In a previous study [1] we have shown that tetracyanoethylene (tcne) also reacts with complex (**1**) to form $[Mo(\equiv CCH_2Bu^t)(\eta^2\text{-}$

Table 2. Bond distances (Å) and selected interbond angles (°) for complex (**11**)

Mo–I	2.856(1)	O(2)–C(2)	1.450(7)	Mo–P(1)	2.457(1)	O(3)–C(3)	1.441(5)
Mo–P(2)	2.444(1)	O(4)–C(4)	1.436(5)	Mo–C(7)	1.927(3)	O(5)–C(5)	1.442(5)
Mo–C(13)	2.370(4)	O(6)–C(6)	1.440(5)	Mo–C(14)	2.441(4)	C(7)–C(8)	1.333(5)
Mo–C(15)	2.362(4)	C(8)–C(9)	1.523(6)	Mo–C(16)	2.246(4)	C(8)–H(8)	0.936(46)
Mo–C(17)	2.251(4)	C(9)–C(10)	1.527(7)	P(1)–O(1)	1.606(3)	C(9)–C(11)	1.529(6)
P(1)–O(2)	1.595(3)	C(9)–C(12)	1.540(7)	P(1)–O(3)	1.618(3)	C(13)–C(14)	1.402(6)
P(2)–O(4)	1.621(3)	C(13)–C(17)	1.446(6)	P(2)–O(5)	1.598(3)	C(14)–C(15)	1.406(7)
P(2)–O(6)	1.606(3)	C(15)–C(16)	1.427(6)	O(1)–C(1)	1.429(5)	C(16)–C(17)	1.436(6)
I–Mo–P(1)	85.3(1)	C(13)–Mo–C(17)	36.4(1)	I–Mo–P(2)	85.6(1)	C(14)–Mo–C(17)	58.7(1)
P(1)–Mo–P(2)	145.0(1)	C(15)–Mo–C(17)	59.8(1)	I–Mo–C(7)	108.9(1)	C(16)–Mo–C(17)	37.2(2)
P(1)–Mo–C(7)	76.2(1)	Mo–P(1)–O(1)	122.7(1)	P(2)–Mo–C(7)	75.0(1)	Mo–P(1)–O(2)	109.9(1)
I–Mo–C(13)	108.4(1)	O(1)–P(1)–O(2)	105.8(2)	P(1)–Mo–C(13)	136.3(1)	Mo–P(1)–O(3)	119.7(1)
P(2)–Mo–C(13)	78.6(1)	O(1)–P(1)–O(3)	96.7(2)	C(7)–Mo–C(13)	131.7(2)	O(2)–P(1)–O(3)	98.7(2)
I–Mo–C(14)	91.8(1)	Mo–P(2)–O(4)	121.0(1)	P(1)–Mo–C(14)	107.5(1)	Mo–P(2)–O(5)	110.3(1)
P(2)–Mo–C(14)	106.5(1)	O(4)–P(2)–O(5)	97.9(2)	C(7)–Mo–C(14)	159.2(2)	Mo–P(2)–O(6)	122.5(1)
C(13)–Mo–C(14)	33.8(1)	O(4)–P(2)–O(6)	96.1(2)	I–Mo–C(15)	107.4(1)	O(5)–P(2)–O(6)	105.6(1)
P(1)–Mo–C(15)	78.7(1)	P(1)–O(1)–C(1)	125.7(3)	P(2)–Mo–C(15)	136.2(1)	P(1)–O(2)–C(2)	122.4(3)
C(7)–Mo–C(15)	133.4(2)	P(1)–O(3)–C(3)	119.0(3)	C(13)–Mo–C(15)	57.6(2)	P(2)–O(4)–C(4)	119.8(3)
C(14)–Mo–C(15)	34.0(2)	P(2)–O(5)–C(5)	122.7(3)	I–Mo–C(16)	143.2(1)	P(2)–O(6)–C(6)	125.6(3)
P(1)–Mo–C(16)	83.7(1)	Mo–C(7)–C(8)	178.2(3)	P(2)–Mo–C(16)	121.7(1)	C(7)–C(8)–C(9)	128.3(3)
C(7)–Mo–C(16)	102.3(1)	C(7)–C(8)–H(8)	120.7(28)	C(13)–Mo–C(16)	60.2(2)	C(9)–C(8)–H(8)	110.9(27)
C(14)–Mo–C(16)	58.8(1)	C(8)–C(9)–C(10)	108.5(4)	C(15)–Mo–C(16)	36.0(1)	C(8)–C(9)–C(11)	110.8(3)
I–Mo–C(17)	144.8(1)	C(8)–C(9)–C(12)	108.7(4)	P(1)–Mo–C(17)	119.9(1)		
P(2)–Mo–C(17)	85.2(1)			C(7)–Mo–C(17)	101.3(1)		

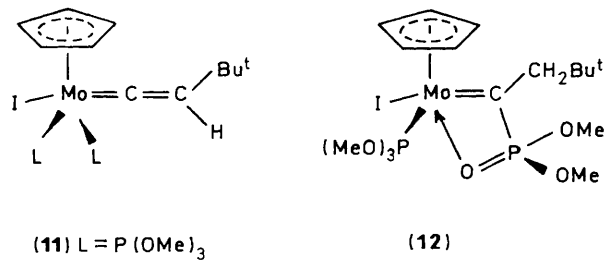

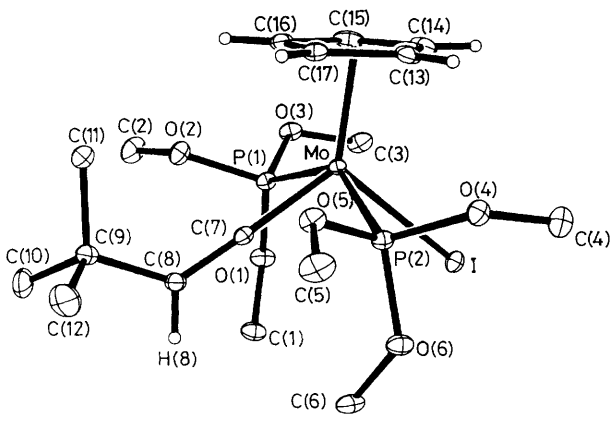

Figure 2. Molecular structure of complex (**11**); atoms are drawn to enclose 30% probability density. Methyl group hydrogen atoms have been omitted for clarity

$C_2(CN)_4\}\{P(OMe)_3\}(\eta\text{-}C_5H_5)]$, and as with the reactions of (**1**) with CO and xylyl isocyanide there is the problem as to how this apparent trimethyl phosphite-displacement reaction occurs. In the case of the tcne reaction it was suggested[1] that a trimethyl phosphite labile species was formed by an initial one-electron-transfer reaction, from the metal-centred highest occupied molecular orbital (h.o.m.o.). This was supported by a cyclic voltammetry experiment in methylene chloride, which showed that (**1**) readily (E_p – 0.11 V) underwent a reversible one-electron oxidation process. This suggested that the carbyne (**1**) might undergo other one-electron oxidative reactions resulting in possible loss of trimethyl phosphite.

Addition of a molar equivalent of $[4\text{-}FC_6H_4N_2][BF_4]$ to a solution of complex (**1**) in CH_2Cl_2 at room temperature resulted in a rapid colour change. In the expectation that the 17-electron $[Mo(\equiv CCH_2Bu^t)\{P(OMe)_3\}_2(\eta\text{-}C_5H_5)][BF_4]$ had been formed diethyl ether was added to the red solution; however, no cationic material was precipitated, but on column chromatography of the reaction mixture on an alumina packed column the dark red neutral crystalline complex (**10**) was obtained. Elemental analysis, i.r., ^1H, $^{13}C\text{-}\{^1H\}$, and $^{31}P\text{-}\{^1H\}$ spectroscopy (see Experimental section) showed that (**10**) was a cyclopentadienyl vinylidene complex carrying a trimethyl phosphite and a three-electron donor diazonium ligand. It is suggested that the addition of (**1**) to the diazonium cation does in fact result in an initial one-electron oxidation reaction to form the sought-for radical cation $[Mo(\equiv CCH_2Bu^t)\{P(OMe)_3\}_2(\eta\text{-}C_5H_5)][BF_4]$. However, before the other product of this electron-transfer reaction, *i.e.* $4\text{-}FC_6H_4N_2^{\bullet}$, can lose N_2, trimethyl phosphite dissociates from the carbyne radical cation to form a 15-electron species, which is captured by $4\text{-}FC_6H_4N_2^{\bullet}$, giving the cationic carbyne $[Mo(\equiv CCH_2Bu^t)(N_2C_6H_4F\text{-}4)\{P(OMe)_3\}(\eta\text{-}C_5H_5)][BF_4]$. Simple proton abstraction from the β-carbon of this cation by free unco-ordinated trimethyl phosphite then affords the isolated vinylidene complex (**10**).

Possibly related reactions occurred between complex (**1**) and CF_3I.* In diethyl ether at room temperature red and green products were formed, these being separated by column chromatography on alumina at low temperature (–30 °C). Elution with hexane afforded a red crystalline complex (**11**) which on the basis of the ^1H, ^{13}C, and ^{31}P n.m.r. spectra could be formulated as a vinylidene, structurally related to *trans*-$[Mo(C{=}CHPh)Br\{P(OMe)_3\}_2(\eta\text{-}C_5H_5)]$.[19] This was confirmed by *X*-ray crystallography; the structure is illustrated in Figure 2 and selected bond lengths and angles listed in Table 2.

* A similar reaction occurred between (**1**) and C_3F_7I, except that an improved (36%) yield of the second product (**12**) was obtained.

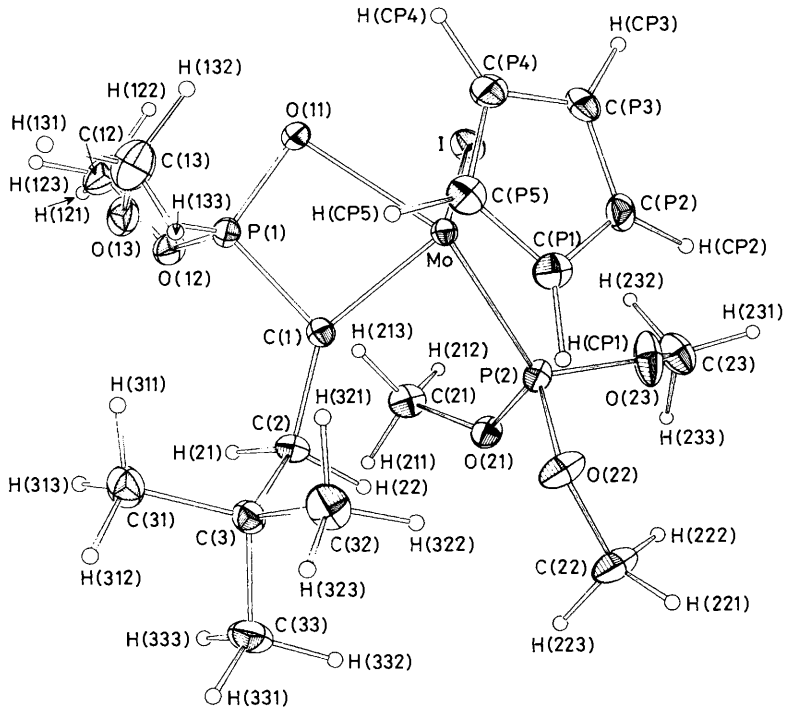

Figure 3. Molecular structure of complex (**12**); details as in Figure 2

The molecule has a four-legged piano-stool geometry with the iodo and vinylidene ligands *trans* to each other. The molybdenum-to-contact carbon bond length [Mo–C(7) 1.927(3) Å] is as predicted[20] theoretically intermediate between Mo≡C triple bond lengths [average 1.80(1) Å] found in carbyne complexes and the formal Mo=C double bonds in the carbene complex $[Mo(CO)_2\{C(OEt)Ph\}(GePh_3)(\eta\text{-}C_5H_5)]$[2.062(11) Å].[21] It is, however, considerably longer than the Mo=C linkage found[22] for the dicyanovinylidene *trans*-$[Mo\{C{=}C(CN)_2\}Cl\{P(OMe)_3\}_2(\eta\text{-}C_5H_5)]$ of 1.83 (1) Å, the shorter bond in this reflecting the greater π-accepting capability of the $C{=}C(CN)_2$ moiety as compared to that of C=CHBu^t. As expected the vinylidene is linear [Mo-C(7)-C(8) 178.2(6)°] with a C(7)-C(8) bond of 1.333(5) Å, *i.e.* of double bond length. The plane of the vinylidene, *i.e.* that through Mo-C(7)-C(8)-C(9), is approximately normal to that of the cyclopentadienyl ring. This contrasts with predictions from extended Hückel molecular orbital (EHMO) calculations[23] on $[Mo(CH_2)(CO)_2(PH_3)(\eta\text{-}C_5H_5)]^+$ allowing for the change from CH_2 to CCHR ligand; however, since the barrier to rotation in vinylidene complexes is likely to be much smaller than for the corresponding alkylidene, *cf.* $[Fe(CH_2)(CO)_2(\eta\text{-}C_5H_5)]^+$ *vs.* $[Fe(CCH_2)(CO)_2(\eta\text{-}C_5H_5)]^+$, the preferred orientation in complex (**11**) is presumably dictated by minimisation of non-bonding interactions between the Bu^t group and the trimethyl phosphite ligands.

Further elution with diethyl ether afforded the second product of the reaction between (**1**) and CF_3I, a green crystalline compound (**12**). Examination of the ^1H, $^{13}C\text{-}\{^1H\}$, and $^{31}P\text{-}\{^1H\}$ n.m.r. spectra (see Experimental section) showed that one of the trimethyl phosphite ligands had undergone an Arbuzov-type reaction. In order fully to understand this type of reaction from a structural standpoint an *X*-ray crystal structure determination was carried out with a suitable crystal of (**12**). This established the structure shown in Figure 3, selected bond lengths and angles being listed in Table 3.

The molecule (**12**) is a molybdenum carbene complex, the Mo–C(1) bond length of 2.006(4) Å being in the range expected for a molybdenum-to-carbon double bond. The dimensions of the four-membered chelate ring $\overbrace{Mo{=}C(1){-}P(1){=}O(11)}$ present in (**12**) may be compared with those of the related fragment $\overbrace{Mn{-}C{-}P{=}O}$ present[24] in the complex $[\overbrace{Mn\{(NC)_2C{=}CP(O)(OPr^i)_2\}}(CO)_2(dppe)]$ (dppe = $Ph_2PCH_2CH_2PPh_2$). Both rings are planar (Σ internal angles = 359.9 and 359.8° respectively) with individual ring angles differing little between the two structures. As might be expected, metal-to-ligand distances are longer in the molybdenum system, but in the case of carbon this increase is somewhat offset by the higher bond order of the Mo–C(1) bond (Δ_{M-O} 0.069, Δ_{M-C} = 0.049Å). The $\eta\text{-}C_5H_5$ ligand is orientated such that it is bisected by a plane constructed through Mo and P(1) perpendicular to the chelate plane. As mentioned above, in $[M(carbene)L_3(\eta\text{-}C_5H_5)]$ complexes where the carbene function is not constrained within a ring system, the complementary relative orientation of the carbene and cyclopentadienyl fragments is found, and has been shown[23] to represent the minimum-energy conformation of a relatively shallow potential well upon rotation. On the opposite side of the four-chain ring lie the iodine and phosphite functions, the latter being *cis* to the carbene function. This provides a steric rationale to the fact that the Bu^t group is found above, if I and P(2) are below, the metallacyclic plane.

The formation of complexes (**11**) and (**12**) from (**1**) is particularly interesting, and it is suggested that their formation is initiated by an initial electron-transfer reaction from the h.o.m.o. of the carbyne (**1**) to R_FI resulting in cleavage of the carbon to iodine bond. As is shown in Scheme 5 such a process would result in the formation of the intermediate (**G**), for which there are two possible reaction paths. One involves abstraction of H$^\bullet$ by the $CF_3^\bullet$ radical to form the vinylidene cation (**H**), which can collapse to form the neutral vinylidene (**11**). The second and more interesting path involves initial abstraction of $CH_3^\bullet$ from a co-ordinated phosphite to form (**I**), which can then undergo charge collapse to form the 18-electron formal

Table 3. Bond lengths (Å) and selected interbond angles (°) for complex (**12**)

Mo–C(P1)	2.231(4)	C(P4)–C(P5)	1.427(7)	P(1)–O(12)	1.575(3)	P(2)–O(23)	1.582(4)
Mo–C(P2)	2.311(4)	C(P5)–C(P1)	1.402(7)	O(12)–C(12)	1.451(6)	O(23)–C(23)	1.368(7)
Mo–C(P3)	2.440(4)	Mo–I	2.822 5(4)	P(1)–O(13)	1.588(3)	C(1)–C(2)	1.518(5)
Mo–C(P4)	2.373(4)	Mo–P(2)	2.430 9(12)	O(13)–C(13)	1.439(6)	C(2)–C(3)	1.552(6)
Mo–C(P5)	2.241(4)	Mo–O(11)	2.226(3)	P(2)–O(21)	1.590(3)	C(3)–C(31)	1.520(7)
C(P1)–C(P2)	1.440(7)	Mo–C(1)	2.006(4)	O(21)–C(21)	1.443(6)	C(3)–C(32)	1.527(7)
C(P2)–C(P3)	1.407(7)	P(1)–O(11)	1.512(3)	P(2)–O(22)	1.597(4)	C(3)–C(33)	1.532(7)
C(P3)–C(P4)	1.384(7)	P(1)–C(1)	1.743(4)	O(22)–C(22)	1.426(6)		
C(P1)–Mo–C(P2)	36.9(2)	P(2)–Mo–C(1)	84.3(1)	P(1)–O(13)–C(13)	120.4(3)	Mo–P(2)–O(22)	111.0(1)
C(P2)–Mo–C(P3)	34.3(2)	C(1)–Mo–O(11)	73.4(1)	P(1)–C(1)–C(2)	123.4(3)	Mo–P(2)–O(23)	119.3(2)
C(P3)–Mo–C(P4)	33.4(2)	O(11)–Mo–I	80.6(I)	Mo–C(1)–C(2)	143.2(3)	O(21)–P(2)–O(22)	101.8(2)
C(P4)–Mo–C(P5)	35.9(2)	C(1)–P(1)–O(11)	102.1(2)	C(1)–C(2)–C(3)	119.8(3)	O(21)–P(2)–O(23)	101.2(2)
C(P5)–Mo–C(P1)	36.5(2)	C(1)–P(1)–O(12)	109.4(2)	C(2)–C(3)–C(31)	112.2(4)	O(22)–P(2)–O(23)	99.9(3)
C(P1)–C(P2)–C(P3)	107.8(4)	C(1)–P(1)–O(13)	122.0(2)	C(2)–C(3)–C(32)	111.1(4)	P(2)–O(21)–C(21)	128.3(3)
C(P2)–C(P3)–C(P4)	108.4(5)	O(11)–P(1)–O(12)	114.3(2)	C(2)–C(3)–C(33)	106.5(4)	P(2)–O(22)–C(22)	125.3(4)
C(P3)–C(P4)–C(P5)	108.6(4)	O(11)–P(1)–O(13)	109.5(2)	C(31)–C(3)–C(32)	109.9(4)	P(2)–O(23)–C(23)	131.3(4)
C(P4)–C(P5)–C(P1)	107.9(4)	O(12)–P(1)–O(13)	100.1(2)	C(31)–C(3)–C(33)	108.4(4)	Mo–O(11)–P(1)	91.5(1)
C(P5)–C(P1)–C(P2)	107.1(4)	P(1)–O(12)–C(12)	121.6(3)	C(32)–C(3)–C(33)	108.5(5)	Mo–C(1)–P(1)	92.9(2)
I–Mo–P(2)	86.63(3)			Mo–P(2)–O(21)	120.5(1)		

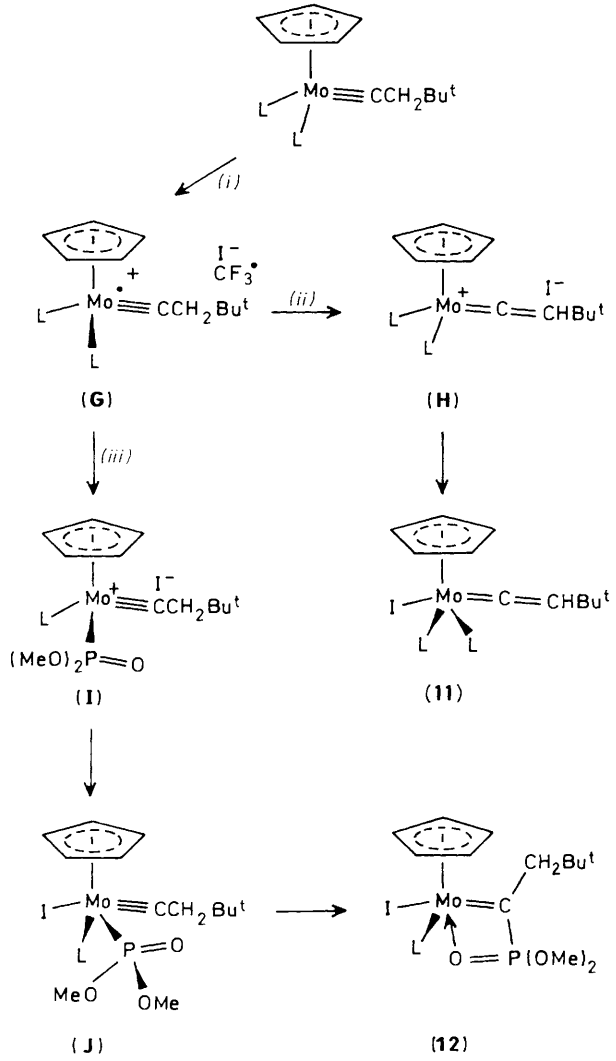

Scheme 5. L=P(OMe)$_3$. (*i*) + CF_3I; (*ii*) − CHF_3; (*iii*) − $CMeF_3$

molybdenum(VI) carbyne complex (**J**). The σ-bonded phosphonate group then migrates from the molybdenum to the carbyne contact carbon atom resulting in the formation of the chelate carbene complex (**12**). This last step is of special interest in that whilst migrations of H,[25] alkyl or aryl[26–28] groups from a metal to a carbene carbon are well known, relatively little is known about related reactions of carbynes, the only well studied system being the reversible migration of hydrogen from a tungsten carbene ($W{=}CH_2$) to form[29] a hydridocarbyne $HW{\equiv}CH$. The formation of (**12**) implies the possibility of a number of such migratory reactions.

Experimental

The ^1H, ^{13}C-{^1H}, and ^{31}P-{^1H} n.m.r. spectra were recorded on JEOL FX 90 Q or FX 200 spectrometers as appropriate. Data are given for room-temperature measurements unless otherwise stated, and coupling constants are in Hz. Chemical shifts are positive to high frequency of the reference, $SiMe_4$ for ^{13}C and ^1H, and H_3PO_4 (85% external) for ^{31}P. I.r. spectra were recorded on a Perkin-Elmer 257 spectrophotometer. All reactions were carried out in Schlenk tubes under an atmosphere of dry oxygen-free nitrogen, using freshly distilled solvents.

Reactions of 2,6-*Xylyl Isocyanide.*—(*a*) *With* [Mo(≡CCH_2-But^t){P(OMe)$_3$}$_2$(η-C_5H_5)]. 2,6-Xylyl isocyanide (0.27 g, 2.0 mmol) was added to a stirred solution of complex (**1**)[30] (0.25 g, 0.51 mmol) in tetrahydrofuran (thf) (5 cm^3) at room temperature. After 12 h the solvent was removed *in vacuo* from the resulting red solution, and the residue extracted with hexane. The hexane extract was chromatographed on an alumina-packed column. Elution with diethyl ether gave an orange band. This was collected and recrystallised (−78 °C) from toluene–hexane to give orange *crystals* of complex (**4**) (0.20 g, 51%) (Found: C, 74.4; H, 8.0; N, 7.4. $C_{47}H_{52}MoN_4$ requires C, 73.4; H, 6.8; N, 7.3%), ν_{NC}(hexane) 2 080s, 2 033s, 2 000(sh), 1 730br, m, and 1 590m cm^{-1}. N.m.r. ($CDCl_3$): ^1H, δ 7.06—6.79 (m, 12 H, $CNC_6H_3Me_2$-2,6), 4.71 (s, 5 H, C_5H_5), 2.28 (s, 12 H, C^1H_3), 2.07* (s, 6 H, C^2H_3), 2.05* (s, 6 H, C^2H_3), 2.03 (s, br, 2 H, CH_2), and 1.23 (s, br, 9 H, CMe_3); ^{13}C-{^1H}, δ 205.4 (s, *C*$NC_6H_3Me_2$-2,6), 189.3 (s, N≡C···*C*···C≡N), 153.2 (s, N≡*C*···C···*C*≡N), 132.7—121.7 ($CNC_6H_3Me_2$-2,6), 88.1 (s, C_5H_5), 48.7 (s, CH_2), 35.7 (s, *C*Me_3), 30.8 (s, C*Me*$_3$), 19.0 (s, C^1H_3), 18.6 (s, C^2H_3), and 18.3 p.p.m. (s, C^2H_3).

* At 44 °C in 1,2,4-trichlorobenzene as solvent these peaks are seen as a singlet at 2.9.

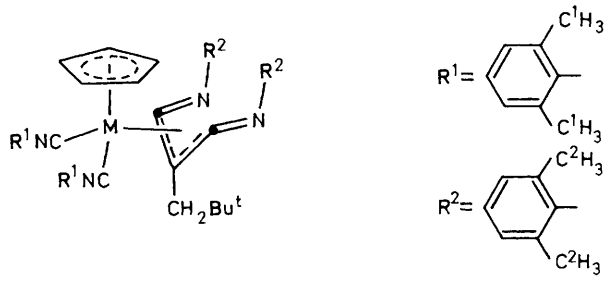

(*b*) *With* [W(≡CCH$_2$Bu^t){P(OMe)$_3$}$_2$(η-C$_5$H$_5$)]. Similarly, reaction for 12 h of complex (**2**)[30] (0.3 g, 0.5 mmol) with 2,6-xylyl isocyanide (0.26 g, 2.0 mmol) in thf (5 cm^3) gave orange *crystals* of (**5**) (0.21 g, 48%) (Found: C, 65.8; H, 6.5; N, 6.4. $C_{47}H_{32}N_4W$ requires C, 65.9; H, 6.1; N, 6.5%), ν_{NC}(CH$_2$Cl$_2$) 2 087s, 2 035s, 1 999(sh), 1 663 br, m, 1 623br, m, and 1 583m cm^{-1}. N.m.r. (CDCl$_3$): ^{1}H, δ 7.08—6.81 (m, 12 H, CNC$_6H_3$Me$_2$-2,6), 4.75 (s, 5 H, C$_5H_5$), 2.30 (s, 12 H, C^{1}H$_3$), 2.19 (s, 2 H, CH$_2$), 2.06* (s, 12 H, C^{2}H$_3$), and 1.25 (s, 9 H, CMe$_3$); ^{13}C-{^{1}H}, δ 177.3 (s, *C*NC$_6$H$_3$Me$_2$-2,6), 173.0 (s, N=C···*C*···C=N), 154.4 (s, N=*C*···C···*C*=N), 132.4—121.5 (CN*C*$_6$H$_3$Me$_2$-2,6), 86.6 (s, C$_5$H$_5$), 48.2 (s, *C*H$_2$), 35.9 (s, *C*Me$_3$), 30.8 (s, C*Me*$_3$), 19.02 (s, C^{1}H$_3$), 18.4 (s, C^{2}H$_3$), and 18.3 p.p.m. (s, C^{2}H$_3$).

(*c*) *With* [Mo(≡CCH$_2$Pr^i){P(OMe)$_3$}$_2$(η-C$_5$H$_5$)][30] (0.29 g, 0.61 mmol) with 2,6-xylyl isocyanide (0.32 g, 2.4 mmol) in hexane (6 cm^3) gave (14 h) after chromatography and recrystallisation (−78 °C) from toluene–hexane red *crystals* of (**6**) (0.27 g, 60%) (Found: C, 73.6; H, 6.7; N, 7.4. $C_{46}H_{50}MoN_4$ requires 73.2; H, 6.6; N, 7.4%), ν_{NC}(CH$_2$Cl$_2$) 2 086m, 2 058s, 2 000(sh), 1 664br, m, 1 647br, m, 1 628br, m, and 1 586m cm^{-1}. N.m.r.: ^{1}H (CDCl$_3$), δ 7.26—6.79 (m, 12 H, CNC$_6H_3$Me$_2$-2,6), 4.87 (s, 5 H, C$_5H_5$), 2.32 (s, 12 H, C^{1}H$_3$), 2.06 (s, 12 H, C^{2}H$_3$), 1.81 (br s, 2 H, CH$_2$), 1.64 (br m, 1 H, C*H*Me$_2$), and 0.90 [d, 6 H, CH*Me*$_2$, ^{3}*J*(HH) 7]; ^{1}H (CD$_2$Cl$_2$, −50 °C), *endo* isomer δ 7.18—6.87 (m, 12 H, CNC$_6H_3$Me$_2$-2,6), 5.38 (s, 5 H, C$_5H_5$), 2.26 (s, 12 H, C^{1}H$_3$), 2.03 (s, 6 H, C^{2}H$_3$), 2.01 (s, 6 H, C^{2}H$_3$), 1.21 [d, 6 H, CH*Me*$_2$, ^{3}*J*(HH) 6.0]; *exo* isomer, 7.18—6.87 (m, 12 H, CNC$_6H_3$Me$_2$-2,6), 5.38 (s, 5 H, C$_5H_5$), 2.49 (s, 12 H, C^{1}H$_3$), 1.98 (s, 12 H, C^{1}H$_3$), 1.98 (s, 12 H, C^{2}H$_3$), and 0.80 [s, 6 H, CH*Me*$_2$, ^{3}*J*(HH) 6.0 Hz] (signals for the CH$_2$ and C*H*Me$_2$ groups could not be conclusively assigned); ^{13}C-{^{1}H} (CDCl$_3$), δ 206.2 (s, *C*NC$_6$H$_3$Me$_2$-2,6), 188.3 (s, N=C···*C*···C=N), 153.4 (s, N=*C*···C···*C*=N), 135.4—121.9 (CN*C*$_6$H$_3$Me$_2$-2,6), 88.6 (s, C$_5$H$_5$), 41.9 (s, CH$_2$), 28.7 (s, *C*HMe$_2$), 23.4 (s, CH*Me*$_2$), 18.9 (s, C^{1}H$_3$), and 18.2 p.p.m. (s, C^{2}H$_3$).

Reaction of Carbon Monoxide with [Mo(≡CCH$_2$Bu^t){P(OMe)$_3$}$_2$(η-C$_5$H$_5$)].—A solution of complex (**1**) (1.0 g, 2 mmol) in hexane (50 cm^3) contained in a glass-liner of a steel autoclave (150 cm^3) was pressurised (300 atm) with carbon monoxide. After 3 d the volatile material was vented, the volume of the solvent reduced *in vacuo*, and the reaction mixture chromatographed on an alumina-packed column. Elution with hexane afforded a yellow band which on crystallisation (−78 °C) from hexane afforded yellow *crystals* of complex (**7**) (0.25 g, 31%) (Found: C, 45.6; H, 6.4%; *M* 396. $C_{15}H_{25}MoO_4P$ requires C, 45.5; H, 6.3%; *M* 396), ν_{CO}(hexane) 1 915s cm^{-1}. N.m.r. (C$_6$D$_6$): ^{1}H, δ 5.25 [d, 5 H, C$_5H_5$, ^{3}*J*(HP) 1.0], 3.40 [d, 9 H, POMe, ^{3}*J*(HP) 12.0], 2.19 [d, 2 H, CH$_2$, ^{4}*J*(HP) 4.5], and 1.06 (s, 9 H, Bu^t); ^{13}C-{^{1}H}, δ 316.3 [d, Mo≡C, ^{2}*J*(CP) 29], 242 [d, CO, ^{2}*J*(CP) 17 Hz], 91.1 (s, C$_5$H$_5$), 51.3 (s, POMe), 63.7 (s, CH$_2$), 32.8 (s, *C*Me$_3$), and 29.7 p.p.m. (s, C*Me*$_3$); ^{31}P-{^{1}H}, δ 203.2 p.p.m. Further elution with diethyl ether–hexane (1:9) gave a second yellow band, which on crystallisation (−78 °C) from hexane gave yellow *crystals* of complex (**8**) (0.21 g, 26%) (Found: C, 52.2; H, 5.2. $C_{13}H_{16}MoO_2$ requires C, 52.0; H, 5.3%), ν_{CO}(hexane) 2 002s and 1 931s cm^{-1}. N.m.r. (C$_6$D$_6$): ^{1}H, δ 5.04 (s, 5 H, C$_5H_5$), 2.15 (s, 2 H, CH$_2$), and 0.94 (s, 9 H, CMe$_3$); ^{13}C-{^{1}H}, δ 332.8 (s, Mo≡C), 229.8 (s, CO), 92.4 (s, C$_5$H$_5$), 64.8 (s, CH$_2$), 33.2 (s, *C*Me$_3$), and 29.5 p.p.m. (s, C*Me*$_3$). Elution with diethyl ether–hexane (1:3) gave unreacted (**1**). Using diethyl ether as eluant gave a further yellow band, which on crystallisation (−78 °C) from hexane gave pale yellow *crystals* of complex (**9**) (0.08g, 8%) (Found: C, 44.6; H, 6.0%; *M* 484. $C_{18}H_{29}MoO_7P$ requires C, 44.5, H, 6.0%; *M* 484), ν_{CO}(hexane) 1 969s, 1 887s, and 1 680m cm^{-1}. N.m.r. (C$_6$D$_6$); ^{1}H, δ 4.92 [d, 5 H, C$_5H_5$, ^{3}*J*(HP) 1.0], 3.68 (s, 3 H, CO$_2$Me), 3.26 [d, 9 H, POMe, ^{3}*J*(HP) 11.5], 3.14 [ddd, 1 H, H^1, ^{3}*J*(H^{1}H^2) 1.0, ^{3}*J*(H^{1}H^3) 12.5, ^{3}*J*(H^{1}P) 5.0], 2.70 [dd, 1 H, H^3, ^{3}*J*(H^{3}H^1) 12.5, ^{2}*J*(H^{3}H^2) 14.0], 1.84 [dd, 1 H, H^2, ^{3}*J* (H^{2}H^1) 1.0, ^{2}*J*(H^{2}H^3) 14.0 Hz], and 1.12 (s, 9 H, C*Me*$_3$). Addition of the opti-shift reagent tris[3-(trifluoromethylhydroxymethylene)-D-camphorato]europium(III) resulted in the CO$_2$*Me* and Bu^t signals appearing as two broad singlets at 3.88, 3.84 and 1.22, 1.20 p.p.m. respectively. The H^1 and H^3 signals were shifted under the POMe signal and H^2 appeared as a broad signal centred at 2.00 p.p.m. ^{13}C-{^{1}H} (C$_6$D$_6$), δ 236.1 [overlapping doublets, CO, ^{2}*J*(CP) 36], 183.4 (s, *C*O$_2$Me), 92.8 (s, C$_5$H$_5$), 52.6 (s, CO$_2$*Me*), 52.3 [d, POMe, ^{2}*J*(CP) 5.0], 49.8 (s, *C*H$_2$Bu^t), 34.1 (s, *C*Me$_3$), 29.5 (s, C*Me*$_3$) and 12.3 p.p.m. [d, *C*HCO$_2$Me, ^{2}*J*(CP) 9.5 Hz]; ^{31}P-{^{1}H}, δ 196.6 p.p.m.

Reaction of 4-*Fluorobenzenediazonium Tetrafluoroborate with* [Mo(≡CCH$_2$Bu^t){P(OMe)$_3$}$_2$(η-C$_5$H$_5$)].—Addition of 4-fluorobenzenediazonium tetrafluoroborate (0.1 g, 0.51 mmol) to a stirred (room temperature) solution of complex (**1**) (0.25 g, 0.51 mmol) in CH$_2$Cl$_2$ (20 cm^3) resulted in a rapid reaction and the formation of a deep red solution. Addition of diethyl ether did not give a precipitate. Removal of the solvent and chromatography on an alumina-packed column gave on elution with hexane–CH$_2$Cl$_2$ (2:1) a deep red band. This was collected and recrystallised (−78 °C) from hexane to give dark red *crystals* of complex (**10**) (0.17 g, 31%) (Found: C, 55.5; H, 5.0. $C_{26}H_{28}FMoN_2O_3P$ requires C, 55.5; H, 5.0%), ν(Nujol) 1 608m and 1 594m cm^{-1}. N.m.r. (C$_6$D$_5$CD$_3$): ^{1}H, δ 7.51 (m, 2 H, FC$_6$H$_4$), 6.92 [t, 2 H, FC$_6$H$_4$, *J*(HH) 8], 5.85 [d, 1 H, C=C*H*Bu^t, ^{4}*J*(HP) 6.0], 5.39 (s, 5 H, C$_5$H$_5$), 3.36 [d, 9 H, POMe, ^{3}*J*(HP) 12.0], and 1.22 (s, 9 H, Bu^t); ^{13}C-{^{1}H}, δ 348.6 [d, Mo=C, *J*(CP) 30.0], 159.4 [d, FC$_6$H$_4$, *J*(CF) 242.0], 146.4 (s, FC$_6$H$_4$), 141.3 (s, C=CHBu^t), 120.5 [d, FC$_6$H$_4$, *J*(CF) 7.0], 115.5 [d, FC$_6$H$_4$, *J*(CF) 25.0], 96.7 [d, C$_5$H$_5$, *J*(CP) 22.0 Hz], 52.0 (s, POMe), 34.7 (s, *C*Me$_3$), and 31.2 p.p.m. (s, C*Me*$_3$); ^{31}P-{^{1}H}, δ 184.7 p.p.m.

Reaction of Trifluoroiodomethane with [Mo(≡CCH$_2$Bu^t){P(OMe)$_3$}$_2$(η-C$_5$H$_5$)].—An excess of CF$_3$I (2.0 mmol) was condensed (−196 °C) into a solution of complex (**1**) (0.25 g, 0.51 mmol) contained in a tube fitted with a Westoff stopcock. The tube and contents were kept at a temperature of −30 °C for 3 d before being allowed to warm to room temperature. The volatile material was removed *in vacuo* and the residue chromatographed on an alumina-packed column retained at −30 °C. Elution with hexane gave a red band which was collected and recrystallised (−20 °C) from hexane to give red *crystals* of complex (**11**) (0.19 g, 30%) (Found: C, 32.7, H, 5.1. $C_{17}H_{33}IMoO_6P_2$ requires C, 32.9, H, 5.3%), ν(Nujol) 1 605m cm^{-1}. N.m.r. (C$_6$D$_6$): ^{1}H, δ 5.31 [t, 1 H, C=C*H*Bu^t, *J*(HP) 13.0], 4.92 [t, 5 H, C$_5H_5$, *J*(HP) 2.0], 3.68 [t, 18 H, POMe, *J*(HP) 5.0], and 1.06 (s, 9 H, Bu^t); ^{13}C-{^{1}H}, δ 326.4 [t, Mo=*C*=CHBu^t, *J*(CP) 51.0], 132.7 [t, C=*C*HBu^t, *J*(CP) 12.0], 91.0 [t, C$_5$H$_5$, *J*(CP) 20.0], 54.5 [t, POMe, *J*(CP) 3.0], 35.0 [t, *C*Me$_3$, *J*(CP)

* At −70 °C in CD$_2$Cl$_2$ this is seen as two signals at δ 2.01 (s, 6 H, C^{2}H$_3$) and 2.00 (s, 6 H, C^{2}H$_3$).

Table 4. Structure analyses[a]

Compound	(4)	(11)	(12)
Crystal data			
Formula	$C_{47}H_{52}MoN_4.xC_6H_{14}$ ($0.0 < x < 0.25$)	$C_{17}H_{33}IMoO_6P_2$	$C_{16}H_{31}IMoO_6P_2$
M	768.9—790.4	618.0	604.2
Crystal system	Triclinic	Monoclinic	Triclinic
Space group (no.)	$P\bar{1}$ (2)	$P2_1/c$ (14)	$P\bar{1}$ (2)
a/Å	12.384(7)	10.362(3)	10.313 0(16)
b/Å	17.669(8)	14.293(4)	12.981 1(3)
c/Å	12.373(5)	16.576(3)	9.191 2(18)
α/°	99.79(4)	90	91.751(17)
β/°	117.85(3)	102.70(2)	106.166(15)
γ/°	97.63(4)	90	94.981(16)
U/Å^3	2 287.7(18)	2 395(1)	1 175.4(1)
T/K	291	250	295
Z	2	4	2
D_c/g cm^{-3}	1.116—1.147	1.71	1.713
$F(000)$	808—833	1 232	600
μ/cm^{-1}	2.7	19.7	18.9
Data collection and reduction			
2θ range/°	2.9—50	4.0—65	2.9—55
Scan speed/ 2θ°min^{-1}	2.4—29.3	2.0—29.3	3.45—5.86
Total data	8 094	6 325	5 445
Unique, 'observed' data, N_0	6 019	5 110	4 419
Observation criterion, n in $F^2 > n\sigma(F^2)$	1	2	2.5
Crystal decay (%)	0	0	25
Absorption correction	None	By azimuthal scans	None
Refinement			
Disordered atoms	Solvent	None	None
Least-squares variables, N_v	266	248	259
R[b]	0.1055	0.044	0.037
R'	0.1107	0.045	0.042
g	0.008 72	0.0002	0.000 557
Difference map features/e Å^{-3}	+1.1 to −1.2	+2.0 to −2.0	+0.7 to −0.9

[a] Details common to all three complexes: λ(Mo-K_α) 0.710 69 Å; graphite monochromator (002); scan method θ—2θ; scan width (2θ) 2.0 + $\Delta_{\alpha_1\alpha_2}$. [b] $R = \Sigma|\Delta|/\Sigma|F_o|$, $R' = \Sigma w^{\frac{1}{2}}\Delta/\Sigma w^{\frac{1}{2}}F_o$, and $\Delta = |F_o| - |F_c|$ where $w = [\sigma_c^2(F_o) + gF_o^2]^{-1}$ and $\sigma_c^2(F_o)$ is the variance in F_o based on counting statistics.

6.0], and 31.3 [t, C*Me*$_3$, *J*(CP) 3.0 Hz]; ^{31}P-{^{1}H}, δ 157.9 p.p.m.

Further elution with diethyl ether afforded a green band, which was collected and recrystallised (−78 °C) from diethyl ether–hexane (1 : 1) to give green *crystals* of complex (**12**) (0.2 g, 35%) (Found: C, 36.5; H, 5.1. $C_{16}H_{31}IMoO_6P_2$ requires C, 36.7, H, 5.1%). N.m.r. (C_6D_6): ^{1}H, δ 4.88 [d, 5 H, C_5H_5, *J*(HP) 3.0], 3.68 [d, 3 H, P(O)OMe, *J*(HP) 10.0], 2.66 [ddd, 2 H, C*H*$_2$Bu^t, *J*(HH) 14.0, *J*(HP) 10.0, 6.0], and 0.96 (s, 9 H, Bu^t); ^{13}C-{^{1}H}, δ 94.5 (s, C_5H_5), 57.9 [dd, *C*H$_2$Bu^t, ^{2}*J*(CP) 9.0, ^{3}*J*(CP) 9.0], 54.8 [d, POMe, *J*(CP) 8.0], 51.2 [d, P(O)OMe, *J*(CP) 9.0], 35.0 (s, *C*Me$_3$), and 30.7 (s, C*Me*$_3$); ^{31}P-{^{1}H}, δ 176.4 [d, P(OMe)$_3$, *J*(PP) 24] and 53.1 p.p.m. [d, P(O)OMe, *J*(PP) 27 Hz].

Structure Analyses of [Mo{η^3-RN=C···C(CH$_2$Bu^t)···C=NR}(CNR)$_2$(η-C_5H_5)] (R = 2,6-$Me_2C_6H_3$) (**4**), [Mo(=C=CHBu^t)I{P(OMe)$_3$}$_2$(η-C_5H_5)] (**11**), *and* [Mo{=C(CH$_2$Bu^t)P(O)(OMe)$_2$}{P(OMe)$_3$}(η-C_5H_5)] (**12**).—Many of the details of the structure analyses carried out on complexes (**4**) (as a hexane solvate), (**11**), and (**12**) are listed in Table 4. *X*-Ray diffraction measurements were made on Nicolet four-circle diffractometers, fitted with an LT-1 crystal cooling device in the case of (**11**). Single crystals were mounted in a thin-walled glass capillary [for (**11**)] or on glass fibres [for (**4**) and (**12**)]. Cell dimensions for each analysis were determined from the setting angle values of 15 centred reflections.

Intensities were collected by θ—2θ scans for unique portions of reciprocal space and corrected for Lorentz, polarisation, crystal decay and, in the case of (**11**), absorption effects. The structures were solved by heavy-atom (direct or Patterson) and Fourier difference methods.

Refinement of complexes (**4**) and (**12**) was by full-matrix, and of (**11**) by blocked-cascade, least squares against F, with all non-hydrogen atoms assigned anisotropic displacement parameters, except for the methyl, solvent, and aromatic, non-ipso, carbon atoms in (**4**). Hydrogen atoms were assigned fixed isotropic displacement parameters and were constrained to ideal geometries with C–H 0.96 Å except for (**12**) in which C–H 1.08 Å. The three unique carbon atoms of the solvent in the structure of (**4**) were assigned occupancies of 0.5 and a common isotropic displacement parameter whose value [0.217(4) Å^2] is indicative of disorder or perhaps lower site occupancy than assigned. Final difference electron-density maps showed no chemically

Table 5. Co-ordinates of refined atoms in complex (**4**)

Atom	*x*	*y*	*z*	Atom	*x*	*y*	*z*
Mo	0.128 98(7)	0.224 87(4)	0.160 32(7)	C(33)	−0.366 1(7)	0.050 4(4)	0.195 5(7)
C(101)	0.076 5(10)	0.115 7(6)	−0.005 0(8)	C(34)	−0.384 4(7)	0.098 8(4)	0.284 0(7)
C(102)	0.182 3(10)	0.170 1(6)	0.012 6(8)	C(35)	−0.299 5(7)	0.171 8(4)	0.358 0(7)
C(103)	0.285 4(10)	0.176 4(6)	0.134 2(8)	C(36)	−0.196 4(7)	0.196 4(4)	0.343 6(7)
C(104)	0.243 2(10)	0.125 9(6)	0.191 8(8)	C(31)	−0.178 1(7)	0.148 0(4)	0.255 0(7)
C(105)	0.114 1(10)	0.088 4(6)	0.105 7(8)	C(32)	−0.263 0(7)	0.075 0(4)	0.181 0(7)
C(1)	0.240 9(8)	0.274 1(5)	0.352 2(9)	C(321)	−0.239 1(14)	0.021 7(9)	0.088 3(13)
N(1)	0.303 0(7)	0.298 9(5)	0.462 4(8)	C(361)	−0.101 4(13)	0.276 8(8)	0.426 2(13)
C(13)	0.469 7(7)	0.428 9(4)	0.788 2(6)	C(4)	−0.013 5(8)	0.279 1(5)	0.042 3(8)
C(14)	0.585 1(7)	0.408 4(4)	0.836 8(6)	N(4)	−0.117 6(7)	0.273 8(4)	−0.055 5(7)
C(15)	0.605 3(7)	0.350 5(4)	0.761 2(6)	C(43)	−0.245 1(8)	0.101 8(4)	−0.336 2(6)
C(16)	0.510 0(7)	0.313 1(4)	0.636 8(6)	C(44)	−0.345 9(8)	0.059 7(4)	−0.331 8(6)
C(11)	0.394 6(7)	0.333 6(4)	0.588 2(6)	C(45)	−0.370 5(8)	0.088 4(4)	−0.235 4(6)
C(12)	0.374 4(7)	0.391 5(4)	0.663 9(6)	C(46)	−0.294 3(8)	0.159 2(4)	−0.143 6(6)
C(121)	0.248 0(11)	0.414 6(7)	0.612 2(11)	C(41)	−0.193 5(8)	0.201 2(4)	−0.148 0(6)
C(161)	0.531 8(15)	0.248 6(9)	0.554 6(15)	C(42)	−0.168 9(8)	0.172 5(4)	−0.244 4(6)
C(2)	0.193 3(8)	0.343 2(4)	0.153 9(7)	C(421)	−0.069 7(13)	0.222 0(8)	−0.260 7(13)
N(2)	0.276 6(7)	0.392 9(4)	0.152 3(7)	C(461)	−0.329 9(12)	0.196 2(8)	−0.047 0(12)
C(23)	0.601 7(5)	0.364 9(5)	0.276 0(5)	C(5)	0.076 6(8)	0.344 3(5)	0.149 7(7)
C(24)	0.601 3(5)	0.337 7(5)	0.163 1(5)	C(6)	0.053 6(9)	0.393 6(5)	0.246 8(8)
C(25)	0.493 3(5)	0.328 6(5)	0.047 0(5)	C(61)	0.026 1(9)	0.474 5(5)	0.227 4(9)
C(26)	0.385 8(5)	0.346 8(5)	0.043 9(5)	C(611)	0.006 9(13)	0.515 1(8)	0.337 5(13)
C(21)	0.386 3(5)	0.374 0(5)	0.156 8(5)	C(612)	0.139 2(14)	0.527 7(9)	0.231 9(13)
C(22)	0.494 2(5)	0.383 1(5)	0.272 8(5)	C(613)	−0.093 0(14)	0.461 4(9)	0.097 2(14)
C(221)	0.502 4(11)	0.423 8(7)	0.396 7(11)	CS(1)	−0.052(5)	−0.022(4)	0.479(7)
C(261)	0.273 0(12)	0.343 4(8)	−0.085 7(12)	CS(2)	−0.134(7)	−0.084(4)	0.457(6)
C(3)	−0.005 0(8)	0.195 1(5)	0.207 3(9)	CS(3)	−0.221(6)	−0.146(4)	0.387(6)
N(3)	−0.078 5(8)	0.174 7(5)	0.238 2(8)				

Table 6. Atomic co-ordinates (× 10^4) for complex (**11**)

Atom	*x*	*y*	*z*
Mo	1 659(1)	795(1)	2 043(1)
I	1 355(1)	−1 132(1)	1 586(1)
P(1)	346(1)	404(1)	3 064(1)
P(2)	3 834(1)	671(1)	1 706(1)
O(1)	572(3)	−538(2)	3 604(2)
O(2)	423(3)	1 239(2)	3 711(2)
O(3)	−1 246(3)	321(2)	2 775(2)
O(4)	3 986(3)	682(2)	754(2)
O(5)	4 696(3)	1 581(2)	2 015(2)
O(6)	4 803(3)	−202(2)	1 991(2)
C(1)	1 823(4)	−958(3)	3 949(3)
C(2)	−336(5)	1 239(4)	4 349(3)
C(3)	−1 806(4)	−425(3)	2 223(3)
C(4)	3 389(5)	−45(3)	198(3)
C(5)	6 062(4)	1 671(3)	1 963(3)
C(6)	4 940(4)	−706(3)	2 757(3)
C(7)	2 907(4)	897(3)	3 090(2)
C(8)	3 755(4)	994(3)	3 816(2)
C(9)	4 160(4)	1 887(3)	4 307(3)
C(10)	3 956(6)	1 743(4)	5 184(3)
C(11)	3 335(5)	2 718(3)	3 903(3)
C(12)	5 633(5)	2 077(4)	4 340(4)
C(13)	1 352(4)	1 705(3)	821(2)
C(14)	120(4)	1 279(3)	776(3)
C(15)	−361(4)	1 552(3)	1 471(3)
C(16)	575(4)	2 165(3)	1 969(3)
C(17)	1 657(4)	2 268(3)	1 563(2)

Table 7. Fractional co-ordinates (for I, Mo, and P, × 10^5; for C and O, × 10^4) of non-hydrogen atoms in complex (**12**)

Atom	*x*	*y*	*z*
I	7 546(3)	20 855(3)	25 100(3)
Mo	17 874(3)	31 179(2)	41 198(3)
P(1)	13 530(11)	31 204(8)	69 100(11)
P(2)	27 877(12)	16 766(8)	32 647(13)
C(P1)	3 529(5)	4 022(3)	3 601(6)
C(P2)	2 536(5)	3 777(4)	2 156(5)
C(P3)	1 422(6)	4 341(4)	2 116(6)
C(P4)	1 659(5)	4 875(3)	3 505(6)
C(P5)	2 963(5)	4 683(3)	4 439(6)
O(11)	534(3)	3 648(2)	5 563(3)
O(12)	523(3)	2 217(2)	7 469(4)
O(13)	1 754(4)	3 898(2)	8 367(3)
O(21)	2 541(3)	548(2)	3 824(4)
O(22)	4 405(4)	1 870(3)	3 780(5)
O(23)	2 530(6)	1 434(3)	1 505(4)
C(12)	−689(7)	2 388(5)	7 914(9)
C(13)	2 222(7)	4 963(4)	8 267(7)
C(21)	1 511(5)	158(4)	4 510(7)
C(22)	5 302(6)	1 171(5)	3 472(9)
C(23)	1 777(7)	636(5)	552(6)
C(1)	2 573(4)	2 610(3)	6 191(4)
C(2)	3 617(4)	1 938(3)	7 081(5)
C(3)	4 948(5)	2 453(4)	8 207(5)
C(31)	4 707(6)	2 925(5)	9 631(6)
C(32)	5 647(6)	3 275(5)	7 451(7)
C(33)	5 883(6)	1 591(5)	8 663(7)

significant features, refinements converging smoothly to residuals given in Table 4. The accuracy of the structural determination of complex (**4**) is somewhat lower than we would have hoped for. We assign this primarily to relatively poor crystal quality [reflected in the high estimated standard deviations (e.s.d.s) on cell parameters] and to difficulty in modelling the disordered solvent. Tables 5, 6, and 7 report the positional parameters for the non-hydrogen atoms in the structures of (**4**), (**11**), and (**12**) respectively. Calculations were made with programs of the SHELXTL[31] and SHELX 76 systems. Complex neutral-atom scattering factors were taken from ref. 32.

Acknowledgements

We thank the S.E.R.C. for support, and Dr. M. Murray for assistance with the DANTE pulse sequence.

References

1 Part 44, M. Bottrill, M. Green, A. G. Orpen, D. R. Saunders, and I. D. Williams, *J. Chem. Soc., Dalton Trans.*, 1989, 511.
2 M. Bottrill and M. Green, *J. Am. Chem. Soc.*, 1977, **99**, 5795; S. R. Allen, R. G. Beevor, M. Green, A. G. Orpen, K. E. Paddick, and I. D. Williams, *J. Chem. Soc., Dalton Trans.*, 1987, 591.
3 E. O. Fischer and U. Schubert, *J. Organomet. Chem.*, 1975, **100**, 59.
4 M. Green, A. G. Orpen, and I. D. Williams, *J. Chem. Soc., Chem. Commun.*, 1982, 493.
5 D. S. Gill, P. K. Baker, M. Green, K. E. Paddick, M. Murray, and A. J. Welch, *J. Chem. Soc., Chem. Commun.*, 1981, 986.
6 P. K. Baker, G. K. Barker, M. Green, and A. J. Welch, *J. Am. Chem. Soc.*, 1980, **102**, 7811.
7 E. O. Fischer, A. R. Ruhs, and F. R. Kreissl, *Chem. Ber.*, 1977, **110**, 805.
8 E. O. Fischer, W. Schambeck, and F. R. Kreissl, *J. Organomet. Chem.*, 1979, **169**, C27.
9 J-M. Bassett, M. Green, J. A. K. Howard, and F. G. A. Stone, *J. Chem. Soc., Dalton Trans.*, 1980, 1779.
10 See, for example, F. Dawans, J. Dewailly, J. Meunier-Piret, and P. Piret, *J. Organomet. Chem.*, 1974, **76**, 53.
11 G. Hüttner, H. H. Brintzinger, L. G. Bell, P. Friedrich, V. Bejerke, and D. Neugerbauer, *J. Organomet. Chem.*, 1978, **145**, 329; M. Green, J. Z. Nyathi, C. Scott, F. G. A. Stone, A. J. Welch, and P. Woodward, *J. Chem. Soc., Dalton Trans.*, 1978, 1067.
12 G. A. Morris and R. Freeman, *J. Magn. Reson.*, 1978, **29**, 433.
13 F. R. Kreissl, A. Frank, U. Schubert, T. L. Lindner, and G. Hüttner, *Angew. Chem., Int. Ed. Engl.*, 1976, **15**, 632; F. R. Kreissl, P. Friedrich, and G. Hüttner, *ibid.*, 1977, **16**, 102; F. R. Kreissl, K. Eberl, and V. Vedelhoven, *Chem. Ber.*, 1977, **110**, 3782; V. Vedelhoven, K. Eberl, and F. R. Kreissl, *ibid.*, 1979, **112**, 3376.
14 S. R. Allen, R. G. Beevor, M. Green, N. C. Norman, A. G. Orpen, and I. D. Williams, *J. Chem. Soc., Dalton Trans.*, 1985, 435.
15 J. L. Davidson, *J. Chem. Soc., Dalton Trans.*, 1987, 2715 and refs. therein.
16 D. C. Brower, K. R. Birdwhistell, and J. L. Templeton, *Organometallics*, 1986, **5**, 94.
17 R. Hoffmann, *Angew. Chem., Int. Ed. Engl.*, 1982, **21**, 711.
18 C. Wilcox and R. Breslow, *Tetrahedron Lett.*, 1980, **21**, 3241.
19 R. G. Beevor, M. Green, A. G. Orpen, and I. D. Williams, *J. Chem. Soc., Dalton Trans.*, 1987, 1319.
20 N. M. Kostic and R. F. Fenske, *Organometallics*, 1982, **1**, 974.
21 J. Y. Y. Chan, W. K. Dean, and W. A. G. Graham, *Inorg. Chem.*, 1977, **16**, 1067.
22 R. M. Kirchner and J. A. Ibers, *Inorg. Chem.*, 1974, **13**, 1667.
23 R. Hoffmann and D. L. Lichtenberger, *Organometallics*, 1982, **1**, 180.
24 G. M. Newton, N. S. Pantaleo, R. B. King, and S. D. Diefenbach, *J. Chem. Soc., Chem. Commun.*, 1979, 55.
25 H. W. Turner, R. R. Schrock, J. D. Fellmann, and S. J. Holmes, *J. Am. Chem. Soc.*, 1983, **105**, 4942 and refs. therein.
26 H. Kleitsein, H. Werner, P. Sevhadli, and M. L. Ziegler, *Angew. Chem., Int. Ed. Engl.*, 1983, **22**, 46.
27 P. Jernakoff and N. J. Cooper, *J. Am. Chem. Soc.*, 1984, **106**, 3026.
28 D. L. Thorn and T. H. Tulip, *J. Am. Chem. Soc.*, 1981, **103**, 5984.
29 M. R. Churchill, H. J. Wassermann, H. W. Turner, and R. R. Schrock, *J. Am. Chem. Soc.*, 1982, **104**, 1710.
30 S. R. Allen, R. G. Beevor, M. Green, A. G. Orpen, K. E. Paddick, and I. D. Williams, *J. Chem. Soc., Dalton Trans.*, 1987, 591.
31 G. M. Sheldrick, SHELXTL, An Integrated System for Solving, Refining and Displaying Crystal Structures from Diffraction Data, Revision 4.1, Nicolet Instruments Ltd., Warwick, 1983; SHELX 76, Cambridge, 1976.
32 International Tables for *X*-Ray Crystallography, Kynoch Press, Birmingham, 1974, vol. 4.

Received 20*th June* 1988; *Paper* 8/02434K